Nonconventional Spin Glass Transition in a Chemically Ordered Pyrochlore

D. K. Singh[1,2,3,*] and Y. S. Lee[1]

[1]Department of Physics, Massachusetts Institute of Technology, Cambridge, Massachusetts 02139, USA
[2]NIST Center for Neutron Research, Gaithersburg, Maryland 20874, USA
[3]Department of Materials Science and Engineering, University of Maryland, College Park, Maryland 20742, USA

(Received 23 July 2012; published 10 December 2012)

We report on the study of unusual spin glass properties in the geometrically frustrated pyrochlore $Tb_2Mo_2O_7$, $T_g \simeq 24$ K. The analysis of the nonlinear part of dc and complex susceptibilities, near the glass transition regime, suggests the existence of a statistical distribution of relaxation times in short-range ordered ferromagnetic clusters. In addition, the magnetic spins are not sufficiently frozen below the glass transition temperature, which is apparently responsible for the nonequilibrium scaling behavior of the static critical exponents of nonlinear susceptibilities. Our report is expected to shed new light in understanding the freezing properties of frustrated pyrochlores with short-range ferromagnetic interactions.

DOI: 10.1103/PhysRevLett.109.247201 PACS numbers: 75.40.Cx, 75.40.Gb, 75.50.Lk

Geometrically frustrated magnets have attracted significant attention in recent years because of their intriguing physical and magnetic properties that are often associated to the novel phenomena of spin liquid, spin ice, or the spin glass transition at low temperatures [1–3]. The spin glass state in geometrically frustrated compounds of stoichiometric composition, such as $Tb_2Mo_2O_7$, $Y_2Mo_2O_7$, $Gd_3Ga_5O_{12}$ (GGG) and $SrCr_8Ga_4O_{19}$ (SCGO) [4–7], is of particular interest. The absence of apparent chemical disorder in the underlying lattice does not fit congruently with a conventional understanding of the spin glass phenomenon, which requires the presence of chemical disorder to create a randomly frustrated system [8]. Recent research on understanding the spin glass properties in geometrically frustrated compounds with antiferromagnetic ground states, such as $Y_2Mo_2O_7$, has suggested the presence of uncompensating magnetic interactions coupled with random strains in the compound as the possible cause of this unusual behavior [9]. However, the proposed theoretical interpretation does not explain the spin glass properties in geometrically frustrated compounds with short-range ferromagnetic order, for example, $Tb_2Mo_2O_7$ ($T_g \simeq 24$ K) [4,10–12].

Despite a lot of effort, very little is known about the spin glass phenomenon in $Tb_2Mo_2O_7$ [11–13]. A thorough understanding of the spin glass phenomenon in a material requires an analysis of the thermodynamic properties near the glass transition. Here we report on a detailed investigation of the spin glass transition in single crystal $Tb_2Mo_2O_7$ using the nonlinear part of dc and ac susceptibilities measurements. While the analysis of the nonlinear dc susceptibilities allows us to understand the static properties near the spin glass transition, the ac susceptibilities provide important information about the dynamic properties in the spin glass state. The pyrochlore $Tb_2Mo_2O_7$ belongs to the $Fd\bar{3}m$ cubic space group, where both Tb^{4+} and Mo^{3+} sublattices form three-dimensional interpenetrating networks of corner sharing tetrahedra. Neutron scattering measurements on both powder and the single crystal identified ferromagnetically correlated short-range ordered clusters of Tb moments well below the spin glass transition $\simeq 1.5$ K [11–14]. The static moment associated with the short-range order of Tb ions at $T = 1.6$ K was determined to be $\langle M_{\mathrm{Tb}} \rangle \simeq 4.0(5)\mu_B$, significantly smaller than that expected for a free Tb^{3+} ion ($\sim 9.5\mu_B$) [11]. We show that the spin glass transition in $Tb_2Mo_2O_7$ is a nonequilibrium phenomenon, which is driven by the statistical distribution of relaxation times in weakly interacting or independent magnetic clusters. In addition, spins are not sufficiently frozen even at the lowest measurement temperature (2 K), which suggests the presence of active spin dynamics in the spin glass state. Our findings are in direct contrast with the observation of a true equilibrium phase transition in the isostructural pyrochlore compound $Y_2Mo_2O_7$ [5], and can be attributed to the different nature of magnetic interactions in these compounds.

First, we determine the nature of the spin glass transition in $Tb_2Mo_2O_7$ (also see Supplemental Material [15]). In a spin glass, the nonlinear parts of dc susceptibilities are of special importance because of their sensitiveness to the freezing order parameter. Analysis of the nonlinear susceptibilities allows us to verify the thermodynamic (or equilibrium) nature of the spin glass transition. The nonlinear susceptibilities are written as the higher order terms in the following equations [5,8,10]:

$$M/H(T) = \chi_1(T) - \chi_3(T)H^2 + O(H^4), \quad (1)$$

$$= \chi_1(T) - a_3(T){\chi_1}^3 H^2 + O(H^4), \quad (2)$$

$$\chi_n 1(T, H) = 1 - M(T, H)/\chi_1 H, \quad (3)$$

where $\chi_1(T)$ is the linear susceptibility at temperature T, $\chi_3(T)$ is the nonlinear susceptibility, the coefficient

$a_3 = \chi_3/(\chi_1)^3$, and $\chi_n 1$ is the net nonlinear susceptibility. Magnetization data on single crystal $Tb_2Mo_2O_7$ were obtained under conventional field-cooling conditions in the field range of 10–10^4 Oe using a commercial magnetometer. The magnetic field was never decreased during the measurement and the sample was slowly cooled from 70 to 10 K at a rate of 0.01 K/ min . We followed the measurement procedure described in Ref. [5] of slow cooling under constant field, as it reduces the possible artifacts in the measurements due to magnetic hysteresis in the superconducting magnet of the magnetometer. It also allows a direct comparison of the static properties between $Tb_2Mo_2O_7$ and the isostructural spin glass $Y_2Mo_2O_7$. The $\chi_1(T)$ at different temperatures were determined by fitting the M versus H curves at low fields. Because of the slow freezing mechanism of the spin glass compared to the experimental observation time, it was not viable to analyze more than the second order term in the magnetization data. Therefore, Eq. (1) reduces to $\chi_3(T, H)\ H^2 = 1 - M(T, H)/\chi_1 H$. Hence, $\chi_n 1(T, H)$ becomes $\chi_3(T, H)H^2$. In Fig. 1(a), we have plotted the net nonlinear susceptibilities, $\chi_{n1}(T, H)$ at various temperatures as a function of H^2. Since we are interested in understanding the thermodynamic behavior near the spin freezing transition, only experimental data from 40 to $\simeq 24$ K are shown in this figure. The maximum value of the field up to which $\chi_{n1}(T)$ is linear in H^2 decreases rapidly as T approaches T_g. This possibly arises due to the higher order corrections in the net susceptibility [16]. The linear portions of $\chi_{n1}(T)$ at different temperatures were fitted with Eq. (2) to extract the coefficient $a3(T)$.

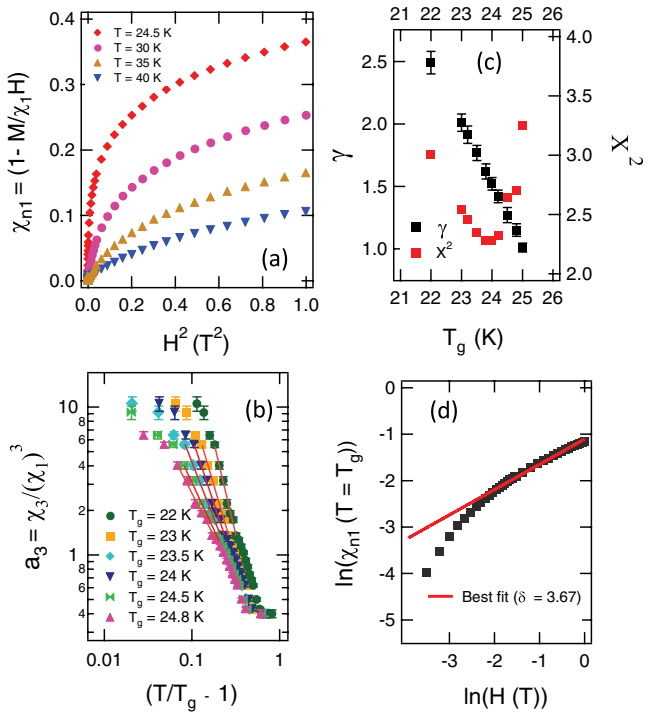

FIG. 1 (color online). (a) Net nonlinear susceptibilities at different temperatures, $\chi_{n1}(T)$, as function of H^2. (b) The temperature dependencies of $a_3 (= \chi_3/\chi_1{}^3)$ on log-log axes for a few different selections of glass transition temperatures. Red curves are the best fits to a subset of the experimental data using Eq. (5) (see text for details). (c) Extracted critical exponent γ and the least square measure of the fitting parameter X^2 are plotted as a function of T_g. A reasonably good fit is obtained at $T_g \simeq 24$ K. (d) Plot of χ_{n1} versus H at $T = T_g$. Red curve is the asymptotic fit to determine another critical exponent δ.

In a conventional spin glass, where the transition is an equilibrium phenomenon, the nonlinear susceptibilities exhibit a scaling behavior according to the single parameter, given by [5,8,10]

$$\chi_{n1}(T, H) = H^{2/\delta} f(\tau^{(\gamma+\beta)/2}/H), \tag{4}$$

where $\tau = (T/T_g) - 1$, γ is the static critical exponent describing the divergent nature of the magnetic susceptibility as a function of temperature and β is the spin glass order parameter critical exponent. Determination of these critical exponents depends on the asymptotic nature of the arbitrary scaling function $f(x)$, with the boundary conditions $f(x) = \text{const}$ as $x \to 0$ and $f(x) = x^{-2\gamma/(\gamma+\beta)}$ as $x \to \infty$. The nonlinear susceptibility, $\chi_{n1}(T, H)$, is expected to follow a power-law dependence in both T and H with two independent static critical exponents γ and δ, respectively. The power law dependencies are described by the following expressions [8,10]:

$$\chi_{n1}(T) \propto \tau^{-\gamma}, \tag{5}$$

$$\chi_{n1}(T = T_g, H) \propto H^{2/\delta}. \tag{6}$$

Typically, the nonlinear susceptibilities diverge as $T \to T_g$ in a conventional spin glass. The two independent exponents, γ and δ, are related to the spin glass order parameter critical exponent β via the following scaling relation:

$$\delta = 1 + (\gamma/\beta). \tag{7}$$

The above scaling relation represents a subtle test, arguably, of the true equilibrium phase transition in a spin glass system.

We use the above formalism to explore the static nature of the spin glass transition in $Tb_2Mo_2O_7$. In Fig. 1(b), we plot a_3 versus τ for a few different choices of glass transition temperatures $T_g \in [22, 25]$ K. For the fitting purpose of Eq. (5), a fixed number of data points on each curve in the divergence regime were selected. As we see in Fig. 1(c), γ is found to vary in the range of [1.1, 2.4]. The best fit is obtained for $T_g = 24$ K with the corresponding value of $\gamma = 1.6$. While the estimated T_g is consistent with the previous dc susceptibility measurements [4,11], the static critical exponent γ is relatively smaller compared to the value ($\gamma \simeq 2.25$) in a conventional spin glass, which exhibits a truly thermodynamic phase transition [5,8,17].

Next, we determine another critical exponent δ by plotting $\ln(\chi_{n1}, T = T_g)$ versus $\ln(H)$ in Fig. 1(d). The best fit of the data using the asymptotic expression of Eq. (6) gives $\delta = 3.67$. If the spin glass transition in $Tb_2Mo_2O_7$ is indeed a true equilibrium phase transition at $T_g = 24$ K, the nonlinear susceptibilities should follow the critical scaling behavior described by Eq. (4). Keeping the value of γ constant, we vary the other critical exponents δ and β systematically to explore the scaling behavior. As shown in Fig. 2, the nonlinear susceptibilities at different temperatures indeed exhibit the scaling collapse on one curve for a set of static critical exponents: $\gamma = 1.6$, $\delta = 4.75$ and $\beta = 1$. At large x values, corresponding to higher temperatures and smaller fields, some data scatter from the scaling curve due to the large errors associated with the smaller nonlinear susceptibilities. Although asymptotic behavior is observed in the scaling plot of Fig. 2, the scaling relation in Eq. (7) is not fulfilled with that set of critical exponents. This suggests the absence of static critical behavior in this compound. This fact, together with the weak divergence of the a_3 coefficient as T_g is approached from above, indicates an unconventional spin glass transition in $Tb_2Mo_2O_7$. The discrepancies in the static critical exponents (between the estimated and the scaling values) leading to the unconventional spin glass behavior can be attributed, arguably, to the formation of small ferromagnetic clusters with short-range order, which ultimately enhances the χ_{n1} considerably and leads to a strong but noncritical background temperature dependence. Similar behavior has been observed in some canonical spin glass systems, which exhibit nonequilibrium transitions [18]. We would like to point out that the spin glass state in $Tb_2Mo_2O_7$ is clearly different from a regular ferromagnet with disorder, as no chemical disorder is found in this compound. Also, the small amount of disorder in an ordered system (a regular ferromagnet) should not affect the phase transition and the associated static critical behavior [19].

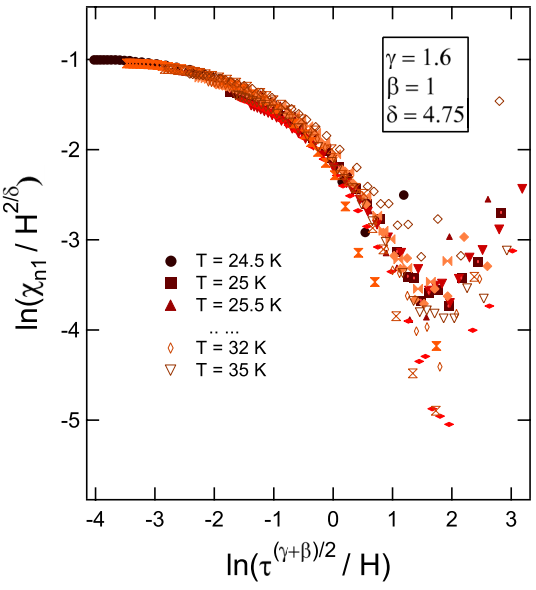

FIG. 2 (color online). Scaling behavior of net nonlinear susceptibilities for a set of critical exponents: $\gamma = 1.6$, $\beta = 1$, and $\delta = 4.75$.

The spin glass transitions in short-range ordered ferromagnetic clusters are often accompanied by a statistical distribution of relaxation times, as each cluster acts as an independent unit [20]. The distribution of spin relaxation times can be extracted from the analysis of the complex (ac) susceptibilities. We have performed complex susceptibility measurements on $Tb_2Mo_2O_7$ using a superconducting quantum interference device in the frequency range of 10–10^4 Hz. The real and imaginary parts of χ at few a characteristic frequencies are plotted in Figs. 3(a) and 3(b). The $\chi'(T)$ curves show typical cusps whose maxima shift to higher temperatures with increasing frequencies, as expected for a spin glass [21]. In addition, χ'' clearly shows a steep rise above zero below $T \leq 26$ K, indicating the existence of a relaxation process in this system. The distribution of spin relaxation times in magnetic clusters is extracted by plotting the real and imaginary parts of the complex susceptibilities in an Argand diagram, as described by the Cole-Cole formalism [22,23]. Accordingly, the complex susceptibility can be phenomenologically expressed as

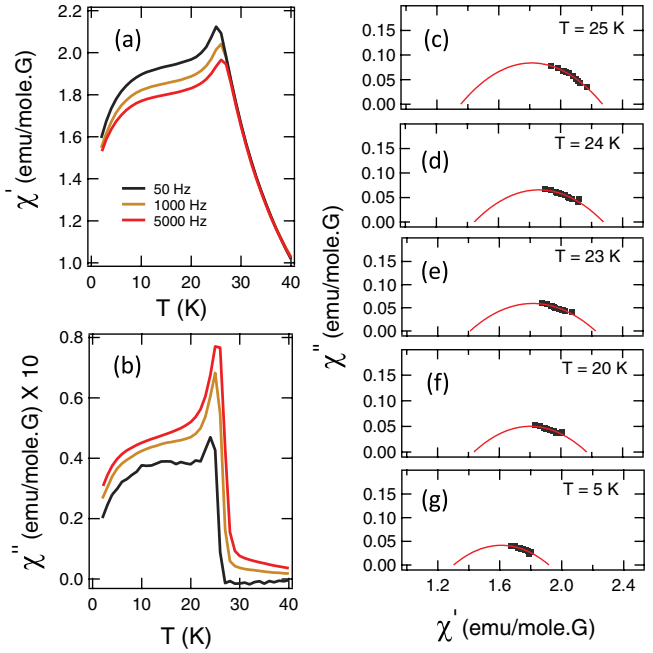

FIG. 3 (color online). (a) and (b) Real and imaginary parts of ac susceptibilities at a few characteristic frequencies. Sharp cusps, indicating the freezing transition, can clearly be seen at all measured frequencies in (a). (c)–(g) Cole-cole diagrams at a few different temperatures across T_g. Solid lines are fit to Eq. (9). The cusp in the real susceptibility moves to higher temperature as the measurement frequency increases.

$$\chi = \chi_s + \frac{\chi_0 - \chi_s}{1 + (i\omega\tau_c)^{1-\alpha}}, \tag{8}$$

where χ_0 and χ_s are the isothermal ($\omega = 0$) and adiabatic ($\omega \to 0$) susceptibilities, respectively, and τ_c is the median relaxation time around which a distribution of relaxation times is assumed. The parameter α determines the width of the distribution, such that $\alpha = 1$ corresponds to an infinitely wide distribution and $\alpha = 0$ returns the Debye equation of a single relaxation time. In the Argand diagram, a single relaxation time is manifested by a perfectly symmetrical full half circle, whereas a distribution of relaxation times in magnetic clusters at temperature T is usually exhibited by a flattened semicircular arc [23]. Equation (8) can be further decomposed into χ' and χ'' to obtain the relations [21]

$$\chi'' = -\frac{\chi_0 - \chi_s}{2\tan[(1-\alpha)\pi/2]} + \sqrt{\left[(\chi_0 - \chi')(\chi' - \chi_s) + \frac{(\chi_0 - \chi_s)^2}{4\tan^2((1-\alpha)\pi/2)}\right]},$$
$$\chi'' = -\frac{\chi_0 - \chi_s}{2}\frac{\cos(\pi\alpha/2)}{\cosh[(1-\alpha)\ln(\omega\tau_c)] + \sin(\pi\alpha/2)}. \tag{9}$$

Argand diagrams of χ'' versus χ' at various temperatures are illustrated in Figs. 3(c)–3(g). We use the first line of Eq. (9) to fit the Argand diagrams in Figs. 3(c)–3(g) with three adjustable parameters, χ_0, χ_s, and α. The maxima of the diagrams give $\omega\tau_c = 1$, while the flatness of the arc is a measure of the width of the distribution of relaxation times. The data points at different frequencies, in these figures, fall on semicircular arcs of varying diameters that tend to flatten as the temperature is reduced. This behavior indicates a distribution of relaxation times in this system. However, unlike some other spin glass systems, the data points at different frequencies do not shift significantly across the maxima in χ'' as the system passes through the spin glass transition. This indicates an unusual spin dynamics feature in $Tb_2Mo_2O_7$, which qualitatively suggests the insufficient freezing of spins well below the glass transition temperature. We determine the actual value of τ_c at each temperature by separately fitting χ'' versus $\ln(\nu)$, as shown in Fig. 4(a)), using the refined values of χ_0, χ_s, and α in the second line of Eq. (9). In the Cole-Cole plots of Figs. 3(c)–3(g), the shape of the arc changes as the temperature is reduced. This clearly indicates that the distribution of relaxation times in magnetic clusters changes with temperature. Similar behavior is observed in the χ'' versus $\ln(\nu)$ plots, where we see an increase in the width of the curves in the vicinity of $T_g = 24$ K. The quantitative measure of the median relaxation time τ_c and its distribution representative, α, are presented in Fig. 4(b) as a function of temperature. Both $\ln(\tau_c)$ and α increase as the temperature is reduced. At $T \leq Tg$, they saturate

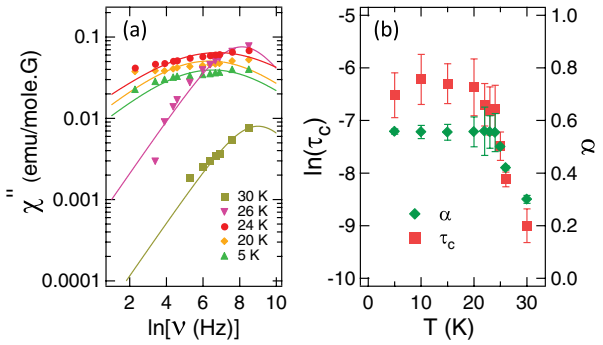

FIG. 4 (color online). (a) χ'' as a function of frequency at several temperatures. The solid lines are fit to the data using Eq. (9) (see text). (b) Temperature dependence of the median relaxation time τ_c and parameter α, reflecting the probability distribution of relaxation times.

around $\simeq -6$ and 0.55, respectively. These analyses indicate that the system is not sufficiently frozen below T_g and significant spin dynamics is still present. It also explains why the spin glass transition in $Tb_2Mo_2O_7$ is a nonequilibrium phenomenon, as depicted earlier by the noncompliance of the scaling law by the static critical exponents deduced from the nonlinear susceptibilities.

In general, a spin glass state arises in a material where the combination of randomness and frustration prevents the development of long-range magnetic order. However, in some materials, such as $Tb_2Mo_2O_7$, $Y_2Mo_2O_7$, or $Gd_3Ga_5O_{12}$, no evidence of chemical disorder is found. We compare our results with some of these unconventional as well as conventional or random spin glasses. The power law divergence coefficient, γ, of the nonlinear susceptibility is found to vary in the range of [2.0, 4.0] in a spin glass compound. Many of them exhibit a thermodynamic transition to the spin glass state; random spin glasses and $Y_2Mo_2O_7$ are notable examples [5,8,17]. However, GGG or SCGO do not exhibit the equilibrium spin glass behavior [6,10]. In these materials, the divergence of χ_{n1} or the scaling behavior were not found to be physically meaningful. The random spin glasses also tends to exhibit complete freezing (i.e., $\alpha \to 1$) as $T \to 0$ K. Our investigation of the spin glass properties in $Tb_2Mo_2O_7$ reveals the nonconventional nature of transition, as manifested by a smaller $\gamma = 1.6$ compared to both conventional and some of the unconventional spin glass systems, a temperature dependent distribution of relaxation times in magnetic clusters and finite spin dynamics below the glass transition. Our results are also consistent with a previous μSR measurement [24], where a significantly smaller relaxation time in the spin glass state, indicating the active presence of spin dynamics, was reported. This behavior is in strong contrast to the conventional spin glass transition in $Y_2Mo_2O_7$, where the magnetic properties are dominated by the antiferromagnetically coupled Mo sublattice only [25]. Because of the small Mo^{4+} moment compared to the

Tb^{3+} moment, the Tb-Tb correlation is the predominant contributor in the magnetic measurements. Recent reports on the study of various possible interactions in this compound suggest that the competition of ferromagnetic or antiferromagnetic interactions (between Tb-Tb and Tb-Mo correlations, or Tb-Tb and Mo-Mo correlations) could be playing a crucial role in the formation of the dynamic spin glass state in $Tb_2Mo_2O_7$ [12,13]. Our results can be useful in understanding the anomalous spin glass transition in other geometrically frustrated pyrochlores with short-range ferromagnetic order, such as $Tb_2Sn_2O_7$ [26] or $Y_2Mn_2O_7$ [27].

The work at MIT was supported by the Department of Energy (DOE) under Grant No. DE-FG02-07ER46134. D. K. S. acknowledges support from the National Science Foundation under Agreement No. DMR-0944772.

*To whom all correspondence should be addressed.
dsingh@nist.gov

[1] J. S. Helton *et al.*, Phys. Rev. Lett. **98**, 107204 (2007).
[2] A. P. Ramirez, A. Hayashi, R. J. Cava, R. Siddharthan, and B. S. Shastry, Nature (London) **399**, 333 (1999).
[3] J. S. Gardner, B. D. Gaulin, S. H. Lee, C. Broholm, N. P. Raju, and J. E. Greedan, Phys. Rev. Lett. **83**, 211 (1999).
[4] B. D. Gaulin, J. N. Reimers, T. E. Mason, J. E. Greedan, and Z. Tun, Phys. Rev. Lett. **69**, 3244 (1992).
[5] M. J. P. Gingras, C. V. Stager, N. P. Raju, B. D. Gaulin, and J. E. Greedan, Phys. Rev. Lett. **78**, 947 (1997).
[6] P. Schiffer, A. P. Ramirez, D. A. Huse, P. L. Gammel, U. Yaron, D. J. Bishop, and A. J. Valentino, Phys. Rev. Lett. **74**, 2379 (1995).
[7] A. P. Ramirez, G. P. Espinosa, and A. S. Cooper, Phys. Rev. Lett. **64**, 2070 (1990).
[8] K. Binder and A. P. Young, Rev. Mod. Phys. **58**, 801 (1986).
[9] A. Andreanov, J. T. Chalker, T. E. Saunders, and D. Sherrington, Phys. Rev. B **81**, 014406 (2010).
[10] B. Martinez, A. Labarta, R. Rodríguez-Solá, and X. Obradors, Phys. Rev. B **50**, 15 779 (1994).
[11] D. K. Singh, J. S. Helton, S. Chu, T. H. Han, C. J. Bonnoit, S. Chang, H. J. Kang, J. W. Lynn, and Y. S. Lee, Phys. Rev. B **78**, 220405(R) (2008).
[12] G. Ehlers, J. R. Stewart, K. C. Rule, P. Fouquet, A. L. Cornelius, C. Adriano, P. G. Pagliuso, Y. Qiu, and J. S. Gardner, Phys. Rev. B **81**, 224405 (2010).
[13] Y. Jiang, A. Huq, C. H. Booth, G. Ehlers, J. E. Greedan, and J. S. Gardner, J. Phys. Condens. Matter **23**, 164214 (2011).
[14] J. E. Greedan, J. N. Reimers, C. V. Stager, and S. L. Penny, Phys. Rev. B **43**, 5682 (1991).
[15] See Supplemental Material at http://link.aps.org/supplemental/10.1103/PhysRevLett.109.247201 for magnetic susceptibility and heat capacity measurements of $Tb_2Mo_2O_7$.
[16] P. Monod and H. Bouchiat, J. Phys. (Paris), Lett. **43**, 45 (1982).
[17] H. Bouchiat, J. Phys. (Paris), Lett. **47**, 71 (1986).
[18] K. Binder, Z. Phys. B **48**, 319 (1982).
[19] S. N. Kaul, J. Magn. Magn. Mater. **53**, 5 (1985).
[20] D. Huser, A. J. van Duyneveldt, G. J. Nieuwenhuys, and J. A. Mydosh, J. Phys. C **19**, 3697 (1986).
[21] A. Mydosh, *Spin Glasses: An Experimental Introduction* (CRC Press, London, 1993), 1st ed.
[22] K. S. Cole and R. H. Cole, J. Chem. Phys. **9**, 341 (1941).
[23] C. Dekker, A. F. M. Arts, H. W. de Wijn, A. J. van Duyneveldt, and J. A. Mydosh, Phys. Rev. B **40**, 11243 (1989).
[24] S. R. Dunsiger *et al.*, Phys. Rev. B **54**, 9019 (1996).
[25] J. Gardner, M. Gingras, and J. Greedan, Rev. Mod. Phys. **82**, 53 (2010).
[26] M. L. Dahlberg, M. J. Matthews, P. Jiramongkolchai, R. J. Cava, and P. Schiffer, Phys. Rev. B **83**, 140410(R) (2011).
[27] J. N. Reimers, J. E. Greedan, R. K. Kremer, E. Gmelin, and M. A. Subramanian, Phys. Rev. B **43**, 3387 (1991).